High-Precision Laser Conditioning of Diamond Grinding Wheels

Norbert Ackerl*, Johannes Gysel, Konrad Wegener

Department of Mechanical Engineering, ETH Zurich, IWF, Leonhardstrasse 21, Zurich, Switzerland

Abstract

A novel approach for machining of cylindrical hard materials and arbitrary shapes is presented. Diamond grinding tools with complex geometry are manufactured with picosecond orthogonal and quasi-tangential combined laser ablation. This rapid and flexible approach for small-scale production of master tools for industrial production trumps conventional approaches. Hitherto, the overall process time is faster compared to conventional technologies with the benefit of free standing diamond grains. A laser manufacturing chain achieving an ablation rate of $35\,\mathrm{mm^3\,min^{-1}}$ with a maximal geometric deviation of 3 µm is presented. The meta-stable diamond structure persists and is assessed via Raman spectroscopy. The final grinding tools is sharpened by a radial laser process removing preferentially the metal-based binding material. This isolates the statistically distributed diamond grains from the binder. Hence, high-precision diamond grinding wheels with a mean error of smaller 1 µm over the complete contour can be manufactured.

Keywords: Diamond grinding tool, laser conditioning, laser manufacturing, ultra-short pulses, Raman spectroscopy, precision machining
2018 MSC: 08-08, 18-19

1. Introduction

The demand for high precision gears to reduce wear and acoustic emission points to the necessity of tight manufacturing tool tolerances. Super-

*Corresponding author. Tel.: +41 44 633 73 50
Email address: ackerln@ethz.ch (Norbert Ackerl)

abrasive like diamond and cubic boron nitrites (cBN) master tools are therefore required to produce hard hobs with long endurance and precision. These master tools are conventionally manufactured by wire electric discharge machining (EDM) or single grain diamond turning. A main drawback of the wire-EDM concerns the non-conductive super-abrasives. The grains are not cut by the wire, but the conductive binder is removed and grains pop out the surface leaving a void. Nevertheless, a defined outer geometry can be produced reaching high precision with the lack of abrasives incorporated. Hence, the grinding tool must be used for some time to set the undefined cutting edges free establishing the demanded high speed grinding process. Laser conditioning has proven to be a viable alternative to the conventional processes and competitive in terms of manufacturing time.

Zhang and Shin (2002) reported in the early 2000s a novel laser assisted truing and dressing technique. A vitrified cBN grinding wheel was produced with a diamond dressing tool in conjunction with a laser. This should increase the life time of the expensive dresser and enable a homogeneous production condition of the grinding wheel. Subsequently, the next logical step of dropping the diamond dresser was reported shortly after, using the laser radiation for truing and dressing. Jackson et al. (2003) introduced an orthogonal dressing process for chromium doped alumina with high power laser Nd:YAG laser. Explicitly, it is stated to use proper laser parameters in terms of power and scan strategy to avoid massive damage. Following, chemical analysis pointed to a resolidified surface with alumina dissolution and chromium oxides. Xie et al. (2004) reported dressing of resin-bonded diamond wheels, where the ablation threshold difference enables an effective sharpening process. However, high precision was not reached due to evaporation of the resin and following loss of the diamond grains. Bronze bonded diamond tools were studied by Hosokawa et al. (2006) and an effective sharpening process with a ms Q-swithced laser. An air jet nozzle is utilized to blow away the metallic binder before resolidification and for low power no damage of the diamond grains observed. However, the established processes were not fast enough to be economically and continuous wave excitation lead to high thermal impact.

Chen et al. (2010) reported laser assisted truing and dressing of bronze-bonded diamond grinding wheels and measured the process forces of such tools. A numerical model to estimate the heat impact during production revealed a non-neglibile amount of graphite at the diamond grains after radial irradiation. Following, Chen et al. (2015) investigated the profiling of comparable tools with a pulsed fibre laser and a tangential process. A de-

fined processing of the grinding wheel was reported with laser power up to 40 W and 210 ns of pulse duration. However, the graphitization of the diamond grain persisted for all parameters with the characteristic Raman peak at 1582 cm^{-1}. A follow up study at the same group (Zhou et al., 2016) investigated the graphitization under ambient, argon and grinding fluid condition. Nonetheless, a graphite layer was clearly detectable in the Raman spectra at all ablation conditions after manufacturing.

von Witzendorff et al. (2012) investigated sharpening and dressing of grinding tools to increase the grain spacing from the binder. Different laser sources with a pulse duration from 12 ps to 20 ns in the near-infrared (1064 nm) and green wavelength (532 nm) regime were assessed. Subsequently, the ablation rate and selectivity studied between binder and diamond grains under a wide parameter set. Short pulses turned out to be beneficial and the statistically distributed diamond grains could be dressed without any detectable phase transition.

Walter et al. (2012) showed laser dressing and truing of cBN grinding tools with high geometric accuracy. A material removal rate of up to 46 mm min^{-3} was reached at 48 W, a pulse overlap 75 % and line overlap 25 %. These parameters pointed to a layer thickness of 50 µm per laser pass keeping the tolerances. Touch dressing of single layer large diamond grains was investigated (Dold et al., 2011) reporting cut diamond grains, which are favorable for high surface quality with small surface roughness. Furthermore, the quality could be increased, if structuring a defined clearance angle on the grains. Transchel et al. (2013) investigated this angle dependence in detail on single diamond grains, which turned out beneficially to alter the cutting characteristics of the tool in terms of smaller forces and workpiece roughness.

A study by Warhanek et al. (2015) pointed out the applicability of laser processing with a laser touch dressing process. The main benefit was a smaller cutting forces at defined clearance angle producible via ultra-short pulsed laser ablation. The inherent self limitation of this process makes the production of high precision geometries feasible. An iterative measurement after subsequent laser manufacturing steps (Warhanek et al., 2017) revealed the potential of high precision fast laser manufacturing for tight tolerances.

Walter et al. (2014) presented laser dressing and truing, which is profiling and sharpening, in detail on industrially used grinding tools. Cleaning and surface structuring techniques were applied to modifiy the tool behavior. Different laser induced profiles studied point to an increased specific material removal rate. However, the wear of the sharpened edges was higher leading

to shorter lifetime and, therefore, higher tool change costs. A similar study was recently presented by Zhang et al. (2018) and reduced cutting forces for structured tools have been reported. The wear started at the laser induced sharp edges leading to round off changing the cutting characteristics.

Within this study combined processes for conditioning of super-abrasive diamond tools are studied. Orthogonal laser ablation is combined with subsequent quasi-tangential incidence conditions. The first leads to high material removal rates and the latter enables high precision manufacturing. A radial finishing process sharpens the precision tool and sets the cutting edges of the super-abrasive grain free from the binding material.

2. Material and Methods

2.1. Experimental Configuration

The ablation setup consisted of five mechanical axes, illustrated in figure 1. A Trumpf TruMicro 5070 regenerative amplified picosecond laser acted as source and was guided via modifying optics into the swivel B axis. Different anti-reflective coated focusing lenses were used to adapt the focal beam diameter and for this study a 150 mm lens leading to a focal radii of 23 µm used. Furthermore, $\lambda/4$ and $\lambda/2$ wave plates allowed to control the polarization state and direction. The X,Y,Z and A axes were driven with controllers from Aerotech Inc. and controlled with Aerotech's A3200 software. The swivel axis B is manually adjusted and not used for the production of grinding wheels, but necessary for e.g. grinding worms. Synchronous defined axes movement of the X,Y,Y and A axis was possible for combined motion. Fast relative surface motion of the laser beam and workpiece was realized with the spindle axis, which operated up to $100\,\mathrm{s}^{-1}$ to adjust the pulse overlap, accordingly. A suction unit with a two stage particle filter (G4, H15) was used to collect the ablation debris. Additionally, an pressurized air operated nozzle at 2 bar was used for convection cooling mounted on the opposite side of the suction unit.

Consequently, a CAM tool set (Gysel, 2017) was developed for the path calculation of orthogonal and quasi-tangential laser manufacturing, which Ackerl et al. (2018) recently reported. Briefly, a CAD file in STL file format can be imported and the axes movement and laser paths are calculated. The setting for the path calculation in the CAM solution has to be determined by a parameter study. Specifically, the layer thickness, beam distance, spindle rotational speed has to be set accordingly. An additional implemented

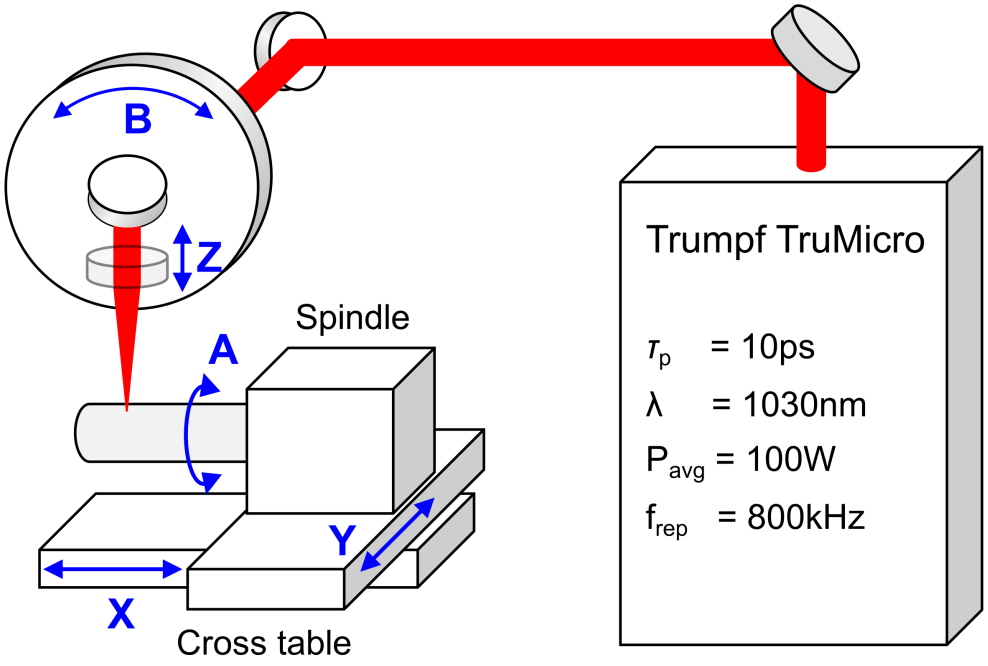

Figure 1: Experimental setup for synchronous laser ablation utilizing an ultrashort-pulsed Trumpf laser source. The axes are three linear stages for XYZ movement, a fast rotating spindle axis A and manual swivel axis B.

feature allows to consider hardware limitations for the axes movements. The maximal speed and acceleration of the axes are defined and the calculated axes movement encompass idle rotations for positioning and accelerating rotations. The latter settings are necessary to take the inertia of the workpiece and axes into account.

2.2. Process Strategies

In general, laser processes have a trade-off between maximal ablation rate, surface quality and dimensional accuracy. Each characteristic can be optimized with an associated parameter set, but in many cases a combination of these characteristics is necessary. Out of this reason three distinct processes are introduced for the laser manufacturing of diamond grinding wheels. An orthogonal roughing processing step is followed by quasi-tangential roughing and finishing. Subsequently, a sharpening step is applied to generated a protrusion of the diamond grains and clean the surface.

Orthogonal laser processes are utilized for high ablation rate and the concept is depicted in figure 2a. The workpiece is rotated with the spindle axis and positioned with the X-axis at the focal position for each layer. Starting with a blank cylinder the layers of depth l_r are ablated with a beam distance l_b on helical paths. The surface speed is controlled by the rotational speed v_r and constantly accelerated for layered ablation to keep the pulse overlap constant at smaller radius. Moreover, the generated flanks project the laser beam and are reflecting parts of the beam. Therefore, a deviation to the designed geometry evolves, which has to be compensated for. In figure 2b the principle of predictive beam path compensation is shown. The laser paths are compensated already in the CAM, where at the flanks a reduced ablation rate is considered by the axial shift of x_c. Additionally, the ablation at the bottom of the contour is shifted radially by r_c to minimize accumulated errors. Both values are attained experimentally and in an iterative manner a quasi-optimum can be found to reach practical dimensional accuracy for the subsequent process steps.

As discussed, the orthogonal roughing process shows a high ablation rate accompanied by low dimensional accuracy. Therefore, a self-limiting quasi-tangential process is subsequently utilized for high precision manufacturing. The laser beam touches the surfaces under grazing incidence, depicted in figure 3a. Surface speed is held constant by controlling the rotational speed v_r and the laser steered synchronized in x and y with a feed rate of v $_\mathrm{f}$. Similar to the orthogonal process the projection of the laser beam on the

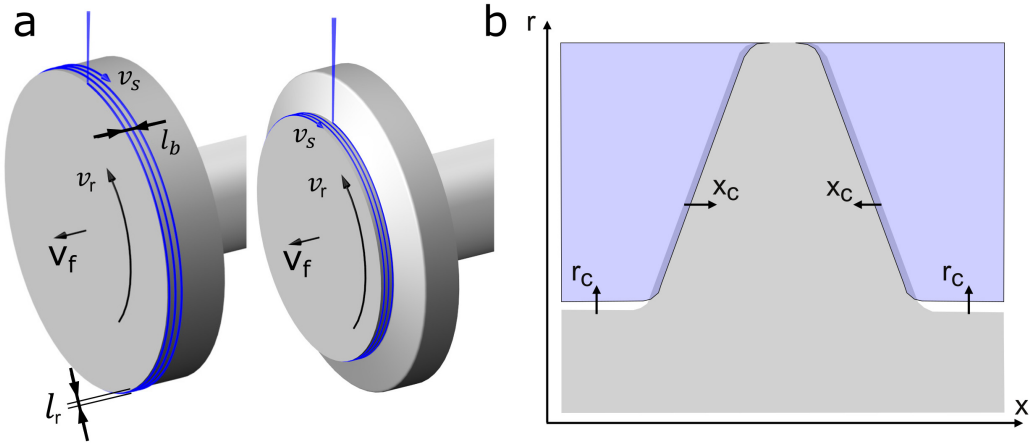

Figure 2: Radial strategy for high ablation rate roughing (a). The laser beam is steered with constant surface speed v_s on helical paths with distance l_b ablating a layer of thickness l_r. In (b) an empirical compensation strategy for radial massive laser ablation process is depicted. The flanks are shifted by x_c and the section with orthogonal incidence moved by r_c.

double curved surface is a challenge and shown in figure 3b. This discrepancy is compensated in the CAM path calculation by lowering the feed rate at the flanks keeping the ablation rate constant.

The last step of the production routine involves an orthogonal sharpening process. This high speed process is carried out with a fast rotation to remove only a small portion of the binding material. A combination of these three processes enables the production of high precision grinding tools in viable time. The distinct calculation of the laser paths without a parameter study is not implemented and would lead to complex computational costly models. Out of that reason a parameter study is carried out to attain the process settings for certain material removal rate and accompanying surface quality. Prospectively, a database will be established for different materials and geometries relying on empirical parameter studies.

2.3. Material

The grinding wheel is supplied by Ultrawheels, a Swiss company specialized in ultra-hard abrasive blanks. The 25 µm natural diamond grains are statistically distributed in a metallic binding material based on copper. The granular mix of binder and diamond grains is heated under pressure well

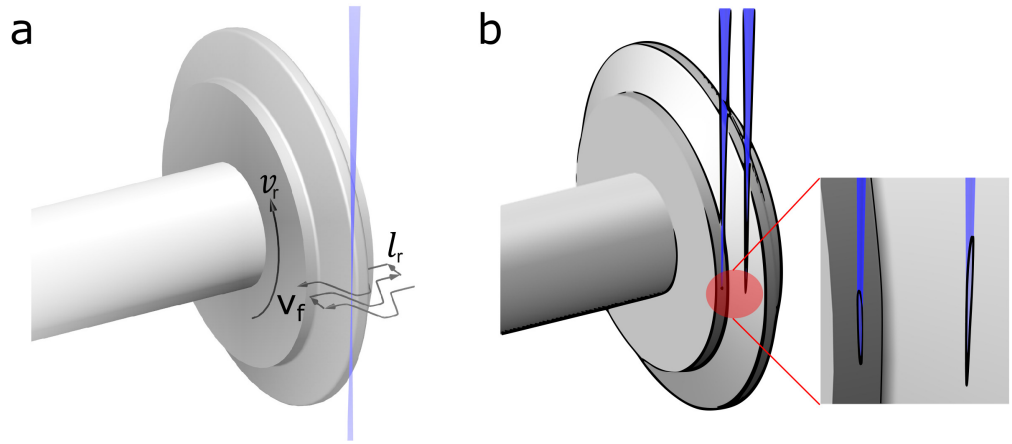

Figure 3: (a) Sketch of the self-limiting quasi-tangential ablation condition and projected laser spot on the flank and bottom. This projection leads to a difference in fluence and is compensated in the laser path calculation. The Laser beam is steered along the contour with v_f, and constant surface speed adjusted by rotational speed v_r.

below the transition temperature of diamond. A 30 mm cylindrical diameter body mounted on a precision grinded cemented carbide shaft is used throughout this study.

2.4. Measurement methods

Optical stereo microscopy was utilized for first inspection after laser manufacturing. A confocal Leica DCM3D $3D$ microscope served as measurement device to determine the depth, ablation volume and surface roughness. Small features and diamond grains were analyzed with a Hitachi SU-70 scanning electron microscope.

Raman spectra were attained with a WITec alpha300R spectroscope and green wavelength of 532 nm. At the used 50x magnification the focal diameter is about 5 µm. The grating was set to 900 cm^{-1} with the spectral center at 1200 nm to measure the Rayleigh peak for calibration. This leads to a measurement range of $-210\,cm^{-1}$ to $2450\,cm^{-1}$ with reasonable signal to noise ratio. Each spectrum was measured five times at the same spot and integrated over 4 s. The measurement data was filtered to remove possible cosmic rays and smoothed by the Savitzky-Golay windowing algorithm.

Geometric preciseness was measured with a Zoller Venturion 450 measurement device. The specimen is illuminated with collimated light and the shadow of the sample is detected by a large scale CCD detector. Two precise

linear axes allow the positioning of the sample and a rotational axis enables the measurement over the whole circumference. The Zoller pilot software was used for evaluation of the measurement and export to a vector file format. An accuracy of 1 µm is specified by the manufacturer.

3. Results and Discussion

3.1. Parameter Study

Two set of parameter studies for the distinct processing strategies has been carried out. Due to the inhomogeneous condition of the blank body with metallic binder and distributed diamond grains single pulse ablation characteristics are not considered. Square pockets with 2 mm side lengths have been ablated on the girthed area of cylinders and on flat specimen of the same material. Hence, a broad parameter range has been experimentally investigated due to limited references on this kind of composite. A first study considered the necessary beam overlap for good surface quality and following was set to 8 µm for both strategies, which is a center point overlap of 83% at a spot size of d_f =46 µm. Figure 4 sums up the study condensed in a two dimensional contour plot.

A trend is revealed with an increase in the ablation rate for higher fluence and lower surface speed. The pulse-to-pulse distance is therefore varied between 3.5 µm and 8.375 µm. The ablation rate depends on a multitude of laser parameters and material properties. In this case the experimental setup and laser source used limit the possible parameter space. A laser wavelength of λ =1030 nm, repetition rate f_rep =800 kHz, pulse duration of τ_p =10 ps and spot size of d_f =46 µm was used. Leaving the average power P and surface speed v_s as adjustable control. Following, the minimal necessary parameters for laser machining are denoted with the adjacent functionality for clarity:

$$\begin{aligned} F &= \frac{P}{w_0^2 \pi f_\mathrm{rep}} = \frac{4P}{d_\mathrm{f}^2 \pi f_\mathrm{rep}} \\ l_\mathrm{p} &= \frac{v_\mathrm{s}}{f_\mathrm{rep}} \\ X_\mathrm{p} &= 1 - \frac{\mathrm{v_f}}{d_\mathrm{f} f_\mathrm{rep}} \\ X_\mathrm{b} &= 1 - \frac{l_\mathrm{b}}{d_\mathrm{f}} \end{aligned} \tag{1}$$

Here additional the pulse X_p and line overlap X_p are given in percent for comparison, which results for the studied surface speed between 80% and 95%. An analytic expression for the ablation rate $\dot{Q}$ cannot be derived straight forward due to the inherent non-linearity of the multi-pulse laser ablation

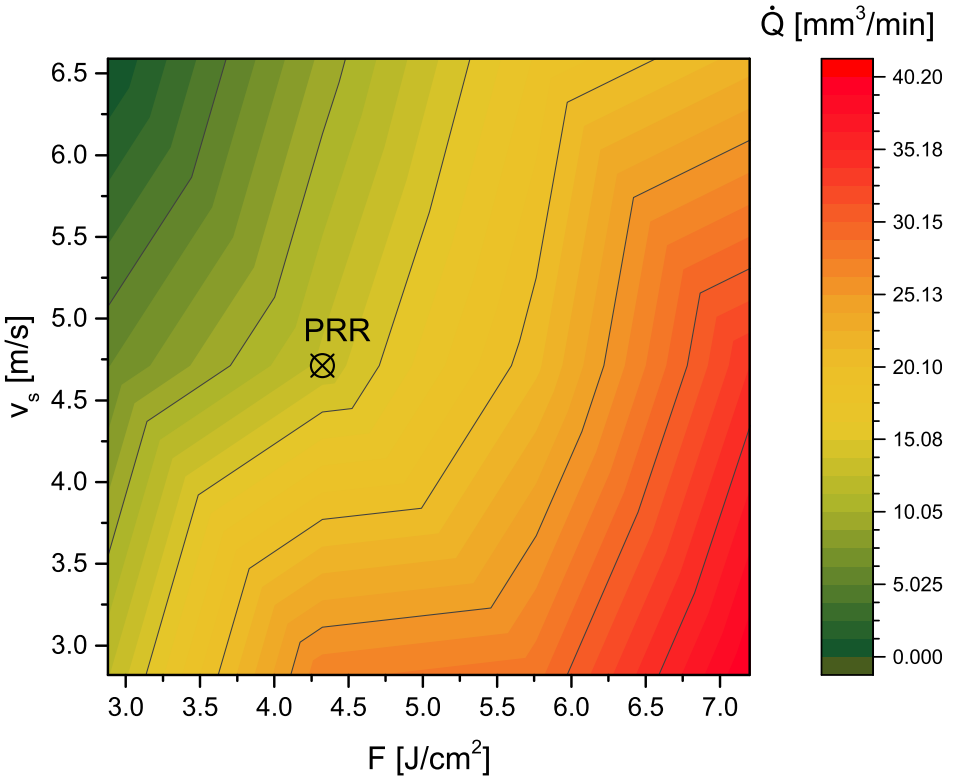

Figure 4: Contour plot of the orthogonal ablation rate depending on the fluence and surface speed, correlated to the pulse overlap. The used parameter set for radial roughing PRR is shown in the graph.

process. However, a proportionality incorporating the angle of incidence θ relative to the surface can be stated to:

$$\dot{Q} \propto (P, f_{\mathrm{rep}}, d_{\mathrm{f}}, v_{\mathrm{s}}, \mathrm{v_f}, \theta) \tag{2}$$

Clearly, the ablation rate strongly differs between the orthogonal and quasi-tangential incidence of the laser radiation. An empirical study reveals the ablation rate and the orthogonal study cannot directly be translated to quasi-tangential processing parameters. Therefore, a separate study has been carried out for these two processes. From the full attained parameters a set in conjunction with maximal ablation rate, surface quality and dimensional accuracy has been selected. Table 1 summarizes the settings for the laser ablation utilized for the laser manufacturing of the diamond grinding wheel.

Table 1: Ablation parameters for different process strategies. Radial roughing PRR, quasi-tangential roughing PTR and finishing PTF and an orthogonal sharpening process PS. The non-projected fluence in the quasi-tangential processes is marked with a $\star$.

Parameter	PRR	PTR	PTF	PS
P [W]	60	100	100	4
F [$\mathrm{J\,cm^{-2}}$]	4.5	$7.52^\star$	$7.52^\star$	0.3
l_{r} [µm]	5.7	10	1	1?
v_{s} [$\mathrm{m\,s^{-1}}$]	4.712	0.188	0.942	2.827
v_{r} [$\mathrm{s^{-1}}$]	50	2	10	30
$\mathrm{v_f}$ [$\mathrm{\mu m\,s^{-1}}$]	400	400	100	500

All parameters reported have been cross checked with the ablation of pockets with defined depth acting as a control. In case of the orthogonal process small deviation in each layer accumulate and point to a higher dimensional deviation.

3.2. Diamond Grinding Wheel

Starting from the blank workpiece diamond grinding wheels were laser manufactured with the described processing strategies and parameters from table 1. In order to compare the processes one grinding tool was manufactured in two parts to study a possible heat affected zone and potential phase transition of the diamond grains. After manufacturing the tool was wire electrical discharge cut, embedded in a conducting polymer and grinded with diamond grinding pads up to grit 4000. The samples have not been

polished preventing the wash out of diamond grains. Subsequently, the cross sectional sample was cleaned with pure ethanol in an ultra-sonic bath for 10 min and rinsed. The cross-section was imaged qualitatively with the SEM and is shown in figure 5. The diamond grains appear blackish and the metallic binder in light grey. Inspection of the cross section points to well distributed diamond grains and no accumulation after laser ablation with high average power. The red horizontal line separates the regions of orthogonal and quasi-tangential ablation without compensation strategies. The bottom

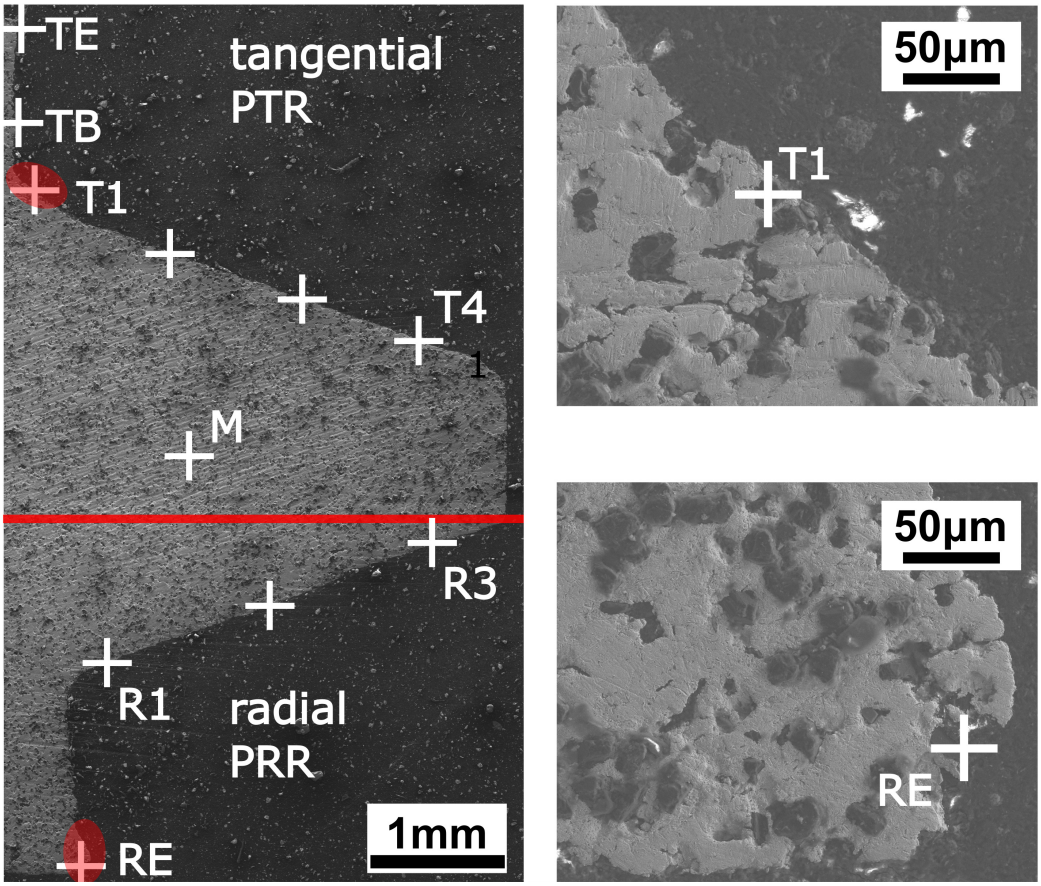

Figure 5: SEM graph of the crosssection after quasi-tangential and radial roughing from a cylindrical blank. The red line separates these two regions. Raman spectra have been taken at each denoted cross to assess possible graphitization. A magnified inset shows the diamond grains in black distributed in the greyish metallic binder.

part of the graph reveals the deviation at the flank and more clearly on the

straight parts of the contour. During the process parts of the beam are deflected at the flank and generate a higher ablated volume. This has been considered for following manufacturing with the compensation strategy presented, compare figure 2b. A magnified SEM graph of two red marked areas reveals the surface condition after ablation. The quasi-tangential manufactured region shows cut diamonds on the edges and the curvature. On the other hand the quality of the orthogonal processed region is lower with higher roughness and deviation. In the SEM analysis no heat affected zone could be detected and the each cross marked diamond grain in figure 5 has been inspected by Raman spectroscopy.

3.2.1. Raman Spectroscopy Study

The Raman spectrum of diamond is well known, having solely one active optical phonon mode. Therefore, the sharp single peak at $1332\,\mathrm{cm}^{-1}$ is easy to detect and can be clearly distinguished by any amorphous or crystalline allotrope of carbon. Crystalline graphite shows a first order single peak at $1575\,\mathrm{cm}^{-1}$ and the amorphous configuration has a broad peak due to the hybridized energy levels centered around the same crystalline peak. Here, the data was analyzed at each of the spots labeled in figure 5 by a least-square fit to the spectral data and a Lorentz peak shape was applied:

$$I = I_0 + \frac{1}{\pi}\frac{2Aw}{4(k-k_\mathrm{c})^2 + w^2}. \tag{3}$$

A constant offset I_0 was taken into account and the peak height A, width w and location k_c fitted. The peak position can give insights into possible laser induced internal stress. However, no peak shift has been detected which is feasible taken into account the soft copper based metallic binder. Figure 6 depicts the measured spectra and the attained Lorentz peak position for the Rayleigh and diamond first order Raman peak. The Rayleigh peak is taken solely for the calibration of the Bragg grating separating the inelastic scattered parts in the instrument. The florescence background in some of the spectra is attributed to the metallic binding material showing some excitation at $1431\,\mathrm{cm}^{-1}$. However, the sharp diamond Raman spectra are clearly distinguishable and no sign of graphite is observed. It can be stated, that high power ultra-short pulsed laser manufacturing up to 100 W does not lead to graphitization. The diamond phase persists for both processing strategies in contrast to longer laser pulses in the nanosecond regime reported previously by Chen et al. (2015).

3.2.2. Dimensional Accuracy and Process Time

The high precision conditioning process involves the fast orthogonal roughing, quasi-tangential roughing and finishing. These three processes allow an accuracy of 10 µm over the complete contour to design. Final finishing is in principle possible if lower fluence is utilized combined with a zero radial feed. In this case the final deviation is solely limited by the precision of the mechanical axes system. Moreover, the quasi-tangential process enables the production of higher precision compared to the focal spot diameter by only coupling a small fraction of the laser beam into the workpiece. However, only scanning the contour takes several tens of passes to reach a quasi-equilibrium ablation state and approaching the final contour. Out of that reason an active compensation has been developed for the quasi-tangential finishing step to reach highest precision in feasible time.

The principal idea of laser path compensation is based on an empirical study. Figure 3b points to the challenge of varying energy density on different regions of the geometry. This leads to changing ablation conditions , therefore, the ablation rate is altered. After the first two processing steps the grinding wheel is measured and the deviation evaluated computationally. The segments to be ablated are overcompensated and the new laser path shifted normal to the contour. A sketch in figure 7a shows the design contour in green and the discretized measurement in blue. Subsequently, the new compensated laser contour is generated for the laser path calculation. Depending on the slope and laser incidence condition the contour is compensated with the empirical attained values. At regions already in tolerance the feed rate is increased to save processing time and no radial feed used. Table 2 shows the processes with the adjacent parameters, number of sliced layers and processing times. After each laser manufactured grinding tools the parameters and compensation values are refined to reach highest precision.

The conditioning process with compensation facilitated a maximal deviation of 3 µm over the whole contour. Moreover, a mean deviation below 1 µm was measured, which indicates a stable manufacturing process and is at the resolution limit of the measurement device. During the manufacturing the metallic binder is preferential ablated, taking into account the lower ablation threshold of metals compared to diamond. Therefore, the final sharpening production step only removes little binder material to set the diamond grains free, but keep enough to have the grains mechanically stable tightened.

Table 2: Number of layers and non-optimized production time. Radial roughing PRR, quasi-tangential roughing PTR and finishing PTF, active compensation PTC and sharpening PS is shown.

Parameter	PRR	PTR	PTF	PTC	PS
P [W]	60	100	100	100	4
v_s [$m\,s^{-1}$]	4.712	0.188	0.942	1.88	2.827
v_f [$\mu m\,s^{-1}$]	400	400	100	100-1000	500
N_{layer} with feed	613	20	30	8	12
N_{layer} no feed	-	5	5	-	-
t_l[s]	9.4	280	111	60	23
t_{proc}[min]	96	100	65	40	5

The process time of the five introduced processes is shown in table 2 for each layer and the process step itself. These times a incorporate the axes movement, positioning and laser ablation. Ultimately, the processes have not been optimized for speed and the manufacturing time can be reduced tremendously. One strong limitation identified is the presented experimental setup, see 1, where the mechanical XY-axes have small acceleration $10\,mm\,s^{-2}$ and maximal velocity of $350\,mm\,s^{-1}$. These side constraints are the reason of an introduced acceleration time and in between two adjacent layers the rotational spindle axis must revolve several time to keep the synchronous movement.

In comparison to conventional production techniques, e.g. diamond dressing, wire-EDM conditioning, the laser manufacturing of diamond grinding wheels is highly competitive. The production time in the presented conditioning process is comparable to industrial used techniques and manufacturing times. Moreover, ultra-short pulsed laser conditioning has the big advantage of being selective on the material and, hence, the diamond grains show a protrusion.

Higher precision and faster manufacturing times are feasible, if an in-line measurement system is utilized, as shown by Warhanek et al. (2017). Ultimately, a orthogonal laser ablation step with higher power can be used and the accumulated errors measured, compensated and high-precision reached with quasi-tangential processing. The measurement can be carried out in principle tactile or contact-free optically. However, the measurement has to be fast to keep the acquisition time of the whole profile low. A viable approach is a laser touch probe with a discretized measurement strategy or an

indirect determination of the process stability with a power meter.

3.2.3. Performance Considerations

The laser conditioned grinding wheels have been tested in an industrially production chain and the tool wear and quality of the hob studied. Additionally, a cemented carbide hob was grinded with conventional wheels for comparison. The total removed volume amounts to more than $8000\,\mathrm{mm}^3$ and revealed highest surface qualitywith a roughness R_a <0.24 µm. Confocal microscopy on the same surface before and after grinding points to negligible wear after the assessed grinding process. Figure 8 shows the measured surface and a line profile reveals the protrusion of the diamond grains.

In strong contrast to conventional production techniques, laser conditioning inherently enables a sharpening of the grinding tool. Albeit, the precision contour can be manufactured by wire-EDM, laser conditioned surfaces contain cut diamond grains protrusion. Exactly, this sharpening process enable a faster grinding processes without pre-grinding of the tool. The reduced initial grinding time to set the grains free of the binder and establishing a cutting edge is one main benefit of the introduced production steps. Moreover, the little wear points to longer tool life time, which reduces tool change costs.

4. Conclusions

A new laser machine tool setup solely build with mechanical has been introduced. The necessary fast surface speed for laser manufacturing is reached with a spindle axis. Following, industrial competitive manufacturing of diamond bonded grinding wheel has been reported. High power ultra-short laser ablation reveals a high potential for the production of master tools to produce precision tools. The three introduced processing steps of roughing, finishing and sharpening allow high precision production within a tolerance band of ±2 µm. In comparison to conventional wire-EDM the processing time is competitive and additionally sharpening is possible.

The manufactured grinding wheels were tested in a real world application and hobs produced. Moreover, the sharpened diamond grinding wheel have a long tool life time and after the production of one hob no wear has been detected. An in-line measurement configuration would allow to speed up the production time and even higher average laser power could be utilized.

Moreover, the ablation rate can tremendously increased if the pulse and line overlap are optimized and the spot diameter enlarged for the roughing step.

Acknowledgements

The authors want to thank the Swiss National Fund [FuSSiT/169654] and the Swiss Commission of Technology and Innovation for the financial support. Access to the SEM at the LMPT and Prof. J.F.Loeffler is appreciated. N.A. wants to personally thank Manuel Beat Leitner for fruitful discussion during the conception of the manuscript.

References

Ackerl, N., Warhanek, M., Gysel, J., Wegener, K., 2018. Path Calculation of 7-axis Synchronous Quasi-Tangential Laser Manufacturing. engrXiv Prepr., 9.
URL https://engrxiv.org/gkhtq/

Chen, G., Deng, H., Zhou, X., Zhou, C., He, J., Cai, S., aug 2015. Online tangential laser profiling of coarse-grained bronze-bonded diamond wheels. Int. J. Adv. Manuf. Technol. 79 (9-12), 1477–1482.
URL http://link.springer.com/10.1007/s00170-015-6963-z

Chen, G., Mei, L., Zhang, B., Yu, C., Shun, K., mar 2010. Experiment and numerical simulation study on laser truing and dressing of bronze-bonded diamond wheel. Opt. Lasers Eng. 48 (3), 295–304.
URL http://www.sciencedirect.com/science/article/pii/S0143816609002796http://linkinghub.elsevier.com/retrieve/pii/S0143816609002796

Dold, C., Transchel, R., Rabiey, M., Langenstein, P., Jaeger, C., Pude, F., Kuster, F., Wegener, K., 2011. A study on laser touch dressing of electroplated diamond wheels using pulsed picosecond laser sources. CIRP Ann. - Manuf. Technol. 60 (1), 363–366.

Gysel, J., 2017. CAM 2.5D Laser Ablation V2.0.
URL https://zenodo.org/record/1048515

Hosokawa, A., Ueda, T., Yunoki, T., jan 2006. Laser Dressing of Metal Bonded Diamond Wheel. CIRP Ann. - Manuf. Technol. 55 (1), 329–332.
URL http://linkinghub.elsevier.com/retrieve/pii/S0007850607604284

Jackson, M. J., Robinson, G. M., Dahotre, N. B., Khangar, A., Moss, R., dec 2003. Laser dressing of vitrified aluminium oxide grinding wheels. Br. Ceram. Trans. 102 (6), 237–245.
URL http://www.tandfonline.com/doi/full/10.1179/096797803225009346

Transchel, R., Heini, F., Stirnimann, J., Kuster, F., Leinenbach, C., Wegener, K., 2013. Influence of the clearance angle on the cutting efficiency of blunt, octahedral-shaped diamonds in an active filler alloy. Int. J. Mach. Tools Manuf. 75, 9–15.

von Witzendorff, P., Moalem, A., Kling, R., Overmeyer, L., 2012. Laser dressing of metal bonded diamond blades for cutting of hard brittle materials. J. Laser Appl. 24 (2), 022002.
URL http://scitation.aip.org/content/lia/journal/jla/24/2/10.2351/1.3685300

Walter, C., Komischke, T., Kuster, F., Wegener, K., 2014. Laser-structured grinding tools - Generation of prototype patterns and performance evaluation. J. Mater. Process. Technol. 214 (4), 951–961.
URL http://dx.doi.org/10.1016/j.jmatprotec.2013.11.015

Walter, C., Rabiey, M., Warhanek, M., Jochum, N., Wegener, K., 2012. Dressing and truing of hybrid bonded CBN grinding tools using a short-pulsed fibre laser. CIRP Ann. - Manuf. Technol. 61 (1), 279–282.
URL http://dx.doi.org/10.1016/j.cirp.2012.03.001

Warhanek, M., Mayr, J., Dörig, C., Wegener, K., dec 2017. Accurate Micro-Tool Manufacturing by Iterative Pulsed-Laser Ablation. Lasers Manuf. Mater. Process. 4 (4), 193–204.
URL http://link.springer.com/10.1007/s40516-017-0046-y

Warhanek, M., Walter, C., Huber, S., Hänni, F., Wegener, K., 2015. Cutting characteristics of electroplated diamond tools with laser-generated positive clearance. CIRP Ann. - Manuf. Technol. 64 (1), 317–320.

URL http://linkinghub.elsevier.com/retrieve/pii/S0007850615000189

Xie, X.-Z., Chen, G.-Y., Li, L.-J., jul 2004. Dressing of resin-bonded superabrasive grinding wheels by means of acousto-optic Q-switched pulsed Nd:YAG laser. Opt. Laser Technol. 36 (5), 409–419.
URL http://linkinghub.elsevier.com/retrieve/pii/S0030399203002032

Zhang, C., Shin, Y., may 2002. A novel laser-assisted truing and dressing technique for vitrified CBN wheels. Int. J. Mach. Tools Manuf. 42 (7), 825–835.
URL http://linkinghub.elsevier.com/retrieve/pii/S0890695502000147

Zhang, X. H., Kang, Z. X., Li, S., Wu, Q. P., Zhang, Z. C., may 2018. Experimental investigations on the impact of different laser macro-structured diamond grinding wheels on alumina ceramic. Int. J. Adv. Manuf. Technol. 96 (5-8), 1959–1969.
URL http://link.springer.com/10.1007/s00170-018-1644-3

Zhou, C., Deng, H., Chen, G., 2016. Study on methods of enhancing the quality, efficiency, and accuracy of pulsed laser profiling. Precis. Eng. 45, 143–152.
URL http://dx.doi.org/10.1016/j.precisioneng.2016.02.005

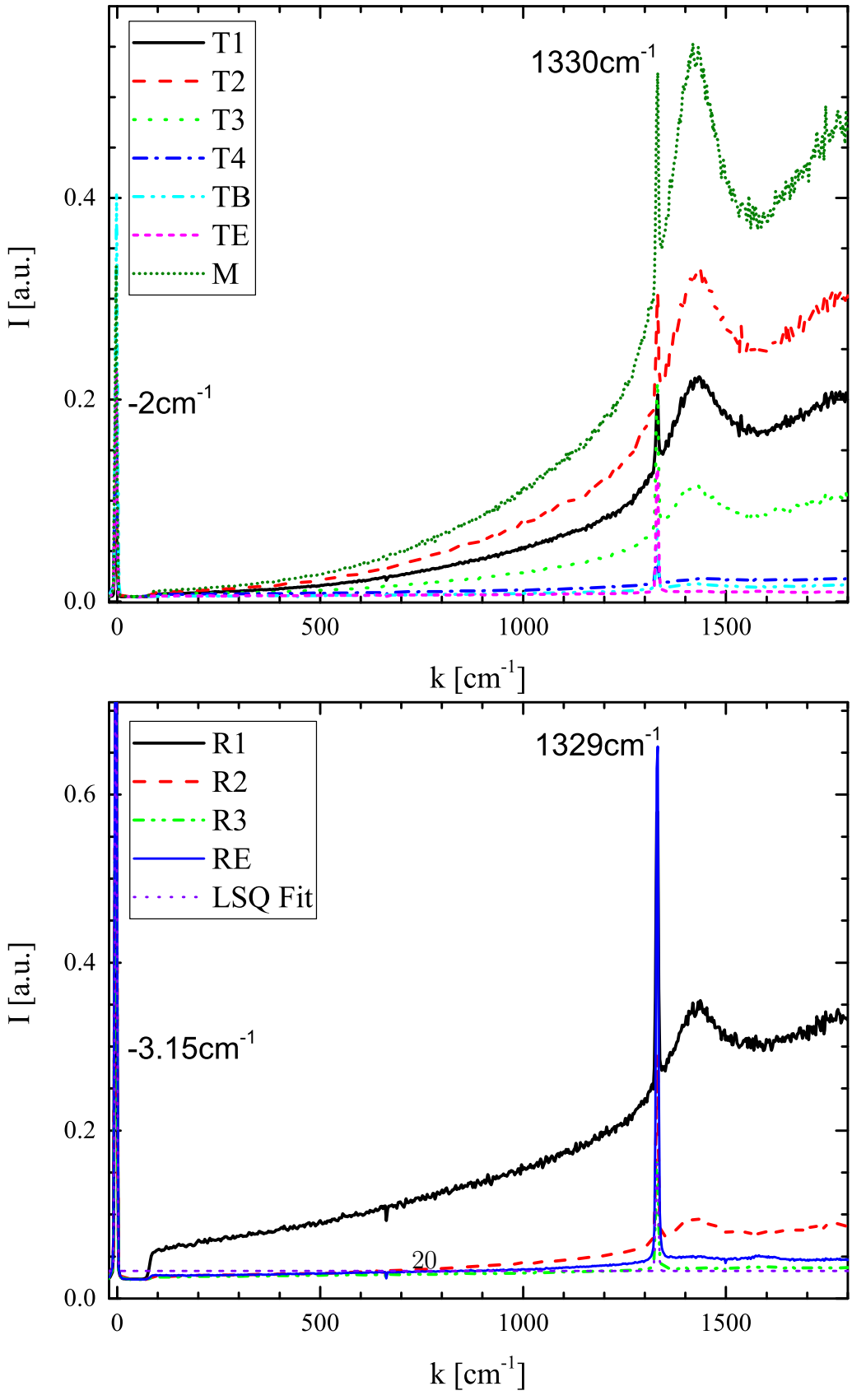

Figure 6: Raman spectra measured after laser machining revealing the diamond structure. The measurement points are denoted after figure 5. A fluorescence background from the

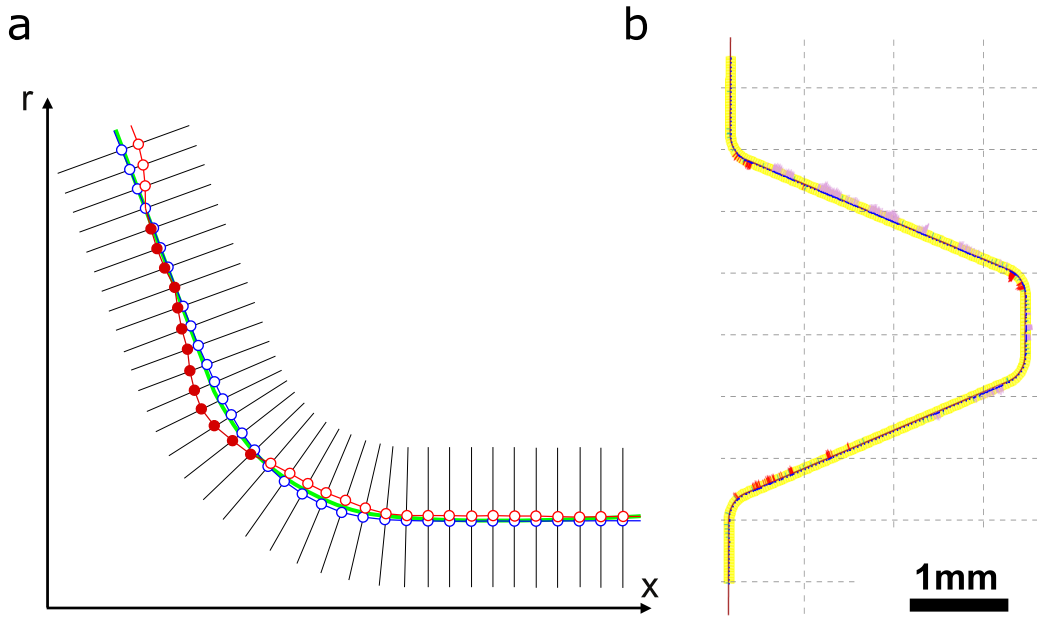

Figure 7: (a) Compensation strategy for high precision with design contour in green and measurement in blue. The red curve shows the orthogonal shifted new laser path. The measured contour over one rotation is shown in (b). A yellow magnified tolerance band with $\pm$ 1.5 µm points to small deviation to design and red sections exceed this tolerance.

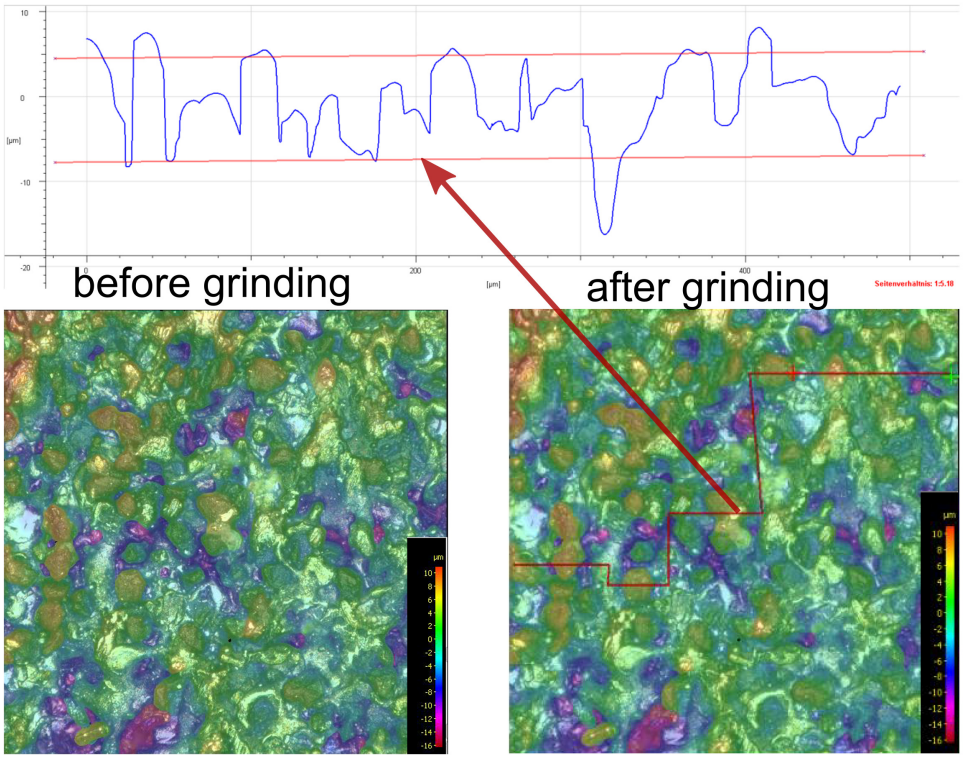

Figure 8: Confocal $3D$ micrographs, Alicona G5 after laser manufacturing left the rolled off surface. After grinding one hob no wear could be detected on the grains. The protrusion persist with about 5um peak and min to max of 12um grain to binder distance.